JOURNAL OF MATERIALS SCIENCE 27 (1992) 6679–6686

Quantification of microcracking in brittle-matrix composites

S. W. YURGARTIS, B. S. MacGIBBON, P. MULVANEY
Center for Advanced Material Processing, Clarkson University, Potsdam, NY 13676, USA

The mechanical properties of brittle-matrix composites are often closely coupled to the generation and propagation of many small cracks. However, the role of microcracking is complex and not well understood on a quantitative basis. Better understanding will require an ability to quantify the crack morphology and how that structure evolves. This paper describes techniques to classify, count and measure the length, spacing and orientation of microcracks. Digital image processing is applied to make the measurements, thereby providing time-effective, reproducible, statistically significant estimates of crack morphology. A key feature of the image processing strategy is to abstract the crack structure to a set of medial axis lines. Proper interpretation of the data requires an understanding of the measurement limitations which are related to size resolution, choice of processing parameters, specimen preparation, and use of sectional views. The techniques are illustrated by data drawn from a carbon–carbon composite laminate. The methods are adaptable to a wide range of materials, and can provide a rich, readily accessible, quantitative description of microcrack structure.

1. Introduction

A fundamental strategy in making viable structural composite materials from brittle constituents is to rely on the generation and propagation of many subcritical cracks to give the material adequate toughness. The complexity and strong coupling of microcracking to thermal and mechanical properties has been widely recognized but is still not well understood. Improved understanding is hampered by (i) an inability to quantify microcracking, (ii) limited observations of microcrack array responses to loads, and (iii) limited evaluations of the mechanics models which propose to explain the role of microcracks. The purpose of this paper is to address the first issue – quantification of microcrack structure. Discussion of how the crack morphology data can be used is beyond the scope of this paper, but it is hoped that the availability of such data will suggest many possibilities related to items (ii) and (iii) above.

A key feature of the techniques described in this paper is the automation of the measurements using computer-aided image processing. The application of image processing methods makes possible time-effective, reproducible measurements of microcrack morphology at sample sizes necessary for statistical confidence and multiple comparisons.

The techniques developed can provide the following measures of crack structure:

(a) Classification of cracks into delamination or transverse bundle cracks.

(b) Number of cracks per unit area. Each microcrack, as a planar intersection, is identified as an individual entity.

(c) Volume fraction of the cracks, and other measures of crack density.

(d) Length of individual cracks and total crack length.

(e) Spacing of adjacent cracks. Typically applied to measure the spacing of transverse bundle cracks within a ply.

(f) Orientation of cracks relative to the principle material directions.

In addition, the raw data have the potential to measure crack width, but this has not yet been developed. Taken together, these measurements provide a rich description of the crack structure.

In this paper particular attention is focused on quantifying cracking in carbon–carbon composites, which typically have a great many microcracks. Carbon–carbons are used as structural composites at extremely high temperatures. Their low density, high stiffness and small CTE also recommend them in many applications. Examples of crack data will be drawn from a carbon–carbon composite. However, the crack measurement techniques given here could be extended to measure microcracking in other brittle matrix composites.

2. Example of a crack structure to be characterized

Fig. 1 is a micrograph of a crack structure of interest, in this case microcracking in a plain-weave reinforced carbon–carbon composite laminate. Microcracks are formed during material production due to CTE mismatches and volumetric shrinkage of the matrix

0022–2461

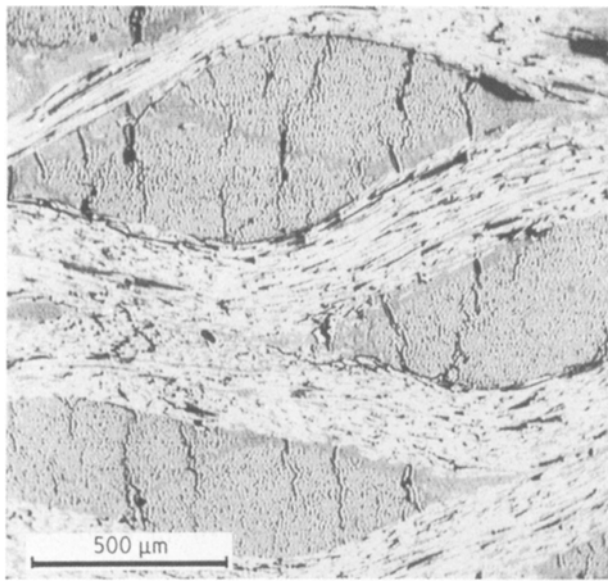

Figure 1 Unprocessed digital image of a carbon–carbon specimen. The carbon fibres appear white, the microcracks are black. This is a plain-weave reinforced laminate; the warp yarns undulate from left to right in the image. The football-shaped fibre bundles are the fill yarns; the fibres are coming "out" of the image.

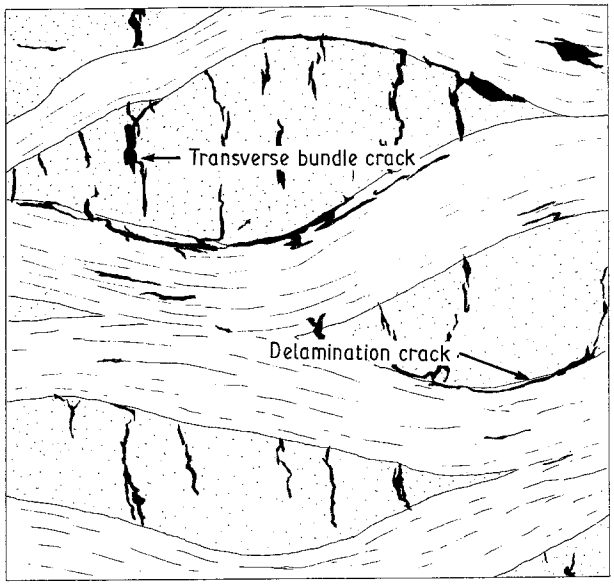

Figure 2 Sketch taken from Fig. 1, highlighting the microcrack structure and defining delamination and transverse bundle crack classifications. The cracks of interest have lengths several times longer than a fibre diameter.

(e.g. during conversion of a pitch to a carbon matrix). It must be noted that in carbon–carbon materials microcracking occurs on many size scales. In the examples, attention will be on characterizing cracks which have a length of the order of a fibre bundle diameter. Magnification of the specimen is chosen accordingly. Cracks on this scale are sometimes referred to as "mini-mechanical" cracks [1], in deference to the finer-scale cracking that occurs at the fibre–matrix interface of individual fibres. Here the bundle-scale cracks are referred to simply as microcracks or cracks.

For this material cracks can be classified into two groups: transverse bundle cracks and delamination cracks (Fig. 2). Transverse bundle cracks are located within the fibre bundles, while delamination cracks are located at the interface between warp and fill fibre bundles. Specimens are viewed in a reference frame where delamination cracks are generally horizontal and transverse bundle cracks are vertical. The two types of crack are likely to react differently to different stress states, and it is desirable to quantify the crack structure of each class independently.

Data, given below, from the example material were obtained by examining sections taken normal to the fill yarn direction. Thus, the longitudinal yarns (running approximately left to right in the images, see Fig. 1) are warp yarns. A typical data set would also include measurements taken from sections normal to the warp yarns. The example data were obtained from 18–20 random but not overlapping images per specimen, which represents a minimum sampled area of 34.8 mm^2.

3. The measurement process

This section outlines how the crack quantification measurements are made. Since a key feature of the technique is automation using image processing techniques, the principles behind the measurements are bound up with the image processing methods used to extract the information. The discussion will therefore follow the sequence used to make the measurements.

The processing involves four major stages: (i) separating the cracks from the background and producing a binary image, (ii) representing the crack structure in an abstracted form, (iii) extracting morphological measurements from the simplified image, and (iv) compensating for sampling biases and providing a statistical description of the measurements.

The technique begins with a microscopic view of a polished specimen surface. Each field of view is converted into a digital image, readily obtained in the examples by mounting a video camera directly on an optical microscope. From this point on, almost all of the process is automated using specially developed image processing and data handling procedures. Successful application of image processing techniques requires attention to many details which are not addressed in this paper. Details can be found in documentation produced with the source code [2].

3.1. Separating the cracks from the background

The original digitized image begins with a 512×480 pixel array of 256 grey levels; Fig. 1 is an example of a starting digital image. The microcracks within this image have good contrast against the matrix and fibre background. Thresholding creates a binary image; inversion of the colours then creates a segmented image with cracks in white and background in black (colours in the figures may have been changed for clarity). The binary image is filtered to eliminate single-pixel "noise"; this noise can be small voids or

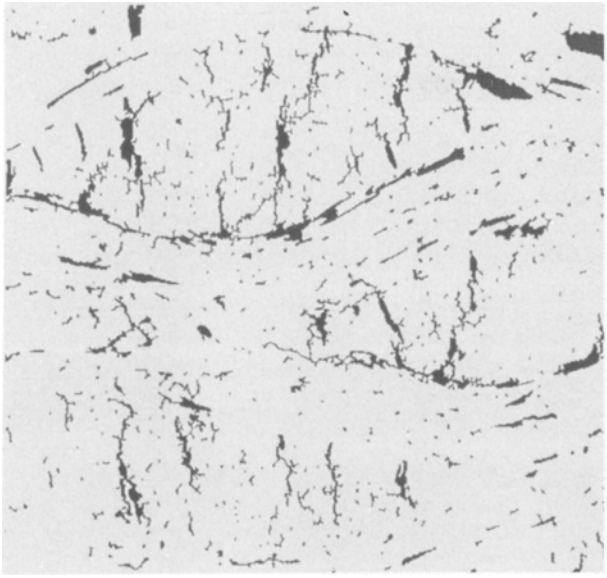

Figure 3 Segmentation of the original image to separate cracks from the background. The image has also been processed to connect broken fragments of cracks. The small black spots are eliminated in subsequent processing.

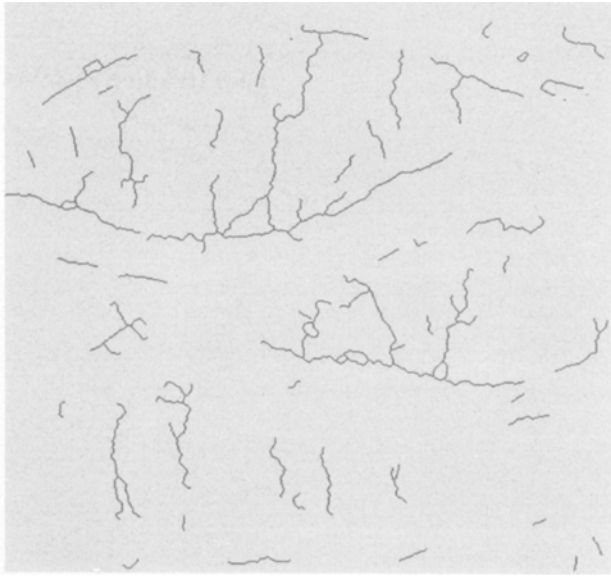

Figure 4 A medial axis representation of the crack structure. Digital image processing has been used to abstract the cracks to a set of lines. These lines retain essential information about the "parent" crack.

cracks that are negligible within the scale of the crack structure of interest.

The thresholded image of the cracks sometimes contains feature degradation due to thickness or colour variation of the original grey-scale image. This can lead to a long crack being represented by a series of smaller crack segments. To compensate, all segments which are separated by less than a specified distance are connected. In the case of the example data given here, the distance is 11 μm, equivalent to 4 pixel lengths. The choice of this spacing is made by comparing the segmented image to the original image. The resulting image is shown in Fig. 3.

At this stage, sometimes with additional noise filtering, it is possible to measure the crack volume fraction using the well-known relationship between area fraction and volume fraction [3]. This is a routine measurement, and provides a vague and global measure of the crack structure.

3.2. Representing the crack structure in an abstracted form: the MAT image

Although the segmented image represents a considerable simplification – and therefore improves the ability to extract information – it is still difficult to quantify crack structure at this stage. A critical next step involves abstracting the crack structure to a set of lines. This is done using a "medial axis transformation" (MAT) [4]. A simple analogy is found in imagining an arbitrarily shaped patch of dried grass which has a grass fire started along the perimeter. As the fire burns, the advancing fire fronts will eventually meet; the meeting line is the medial axis. Abstraction of the cracks to a set of lines greatly simplifies the extraction of morphological data. Each line contains the essential features of the "parent" crack, i.e. length, orientation, spacing and width. Width information is retained by recording the amount of thinning required at each point to arrive at the medial axis. Fig. 4 is the medial axis representation of the crack structure seen in the original image of Fig. 1.

Before the medial axis transformation is started, some prior conditioning of the segmented image is required. The contours of the cracks are normally rough, at least in these materials. Smoothing of the contours results in a better MAT representation of the structure since "bumps" will result in small, inappropriate branches on the medial axis. Smoothing is accomplished by filling in, and cutting off, small contour irregularities. In the example material, irregularities of about 6 μm (or 2 image pixels) in radius were smoothed.

After the MAT, there may yet remain some short branches which do not accurately represent the crack structure. These are removed, if necessary, by eliminating all branches less than some specified length. In the case of the example image, MAT cracks less than 28 μm (10 pixels) were removed. Selection of this length requires a judgement to be made based on comparison of the MAT image with the original image. The selected threshold length becomes constant for all measurements made on similar materials.

The method of producing a MAT abstraction of the crack structure has been developed to the point where it is capable of providing a good representation of the crack structure. Fig. 5 shows the MAT image superimposed upon the original image. The representation is, of course, only valid in a limited size-scale range. Further discussion of detection limits is found below.

4. Extracting information about crack structure

Crack morphology measurements can be extracted from the MAT representation of the crack structure.

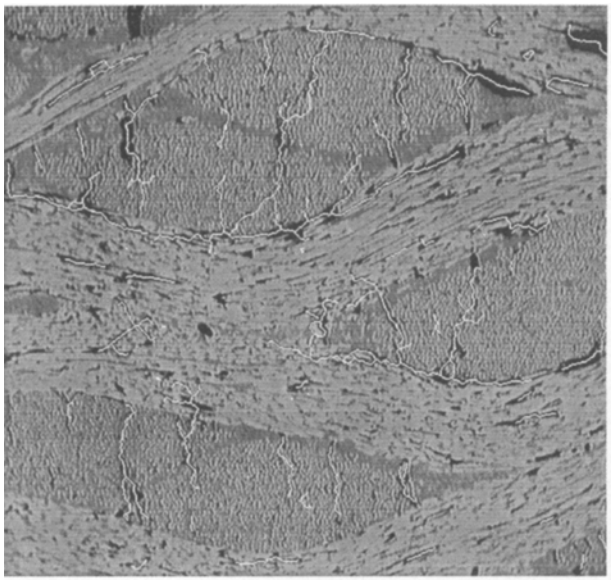

Figure 5 The medial axis representation of the crack structure superposed on the original image. Cracks smaller than 27 μm in length have been discarded. See text for a discussion of resolution.

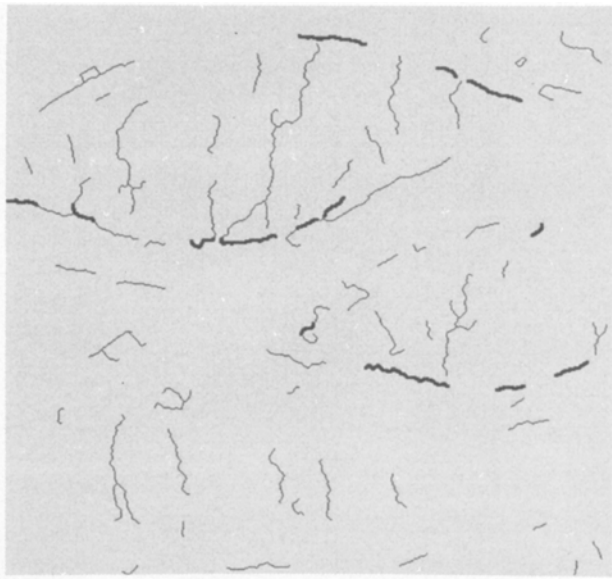

Figure 7 Image showing the automatic classification of cracks into delamination and transverse bundle cracks. Delamination cracks are shown as the bolder black lines.

The following sections describe the various measures that have been developed. Example data, taken from the material shown in Fig. 1, are given in each section.

4.1. Classification of transverse bundle and delamination cracks

Classification is initiated by identifying the interface between longitudinal and transverse fibre bundles. Automation of this step is not yet complete; it is presently accomplished manually using a mouse-and-cursor set-up. Using a cursor, the operator locates 10–20 points along an interface. A seventh-order polynomial is then generated to fit these points, creating a functional representation of the interface. The black lines in Fig. 6 show the functional fits to the yarn interfaces; good fits are obtained. Because a function is smoothed through the points selected by the operator, the method has the advantage of not being acutely sensitive to operator input.

To classify the microcracks, the interface boundaries are overlayed on the MAT representation of the cracks. Cracks that lie within a specified neighbourhood of an interface ($\pm$ 11 μm in the example data) are identified as delamination cracks. The remainder of the cracks are classified as transverse bundle cracks. A crack-classified image can be seen in Fig. 7. To facilitate measurement of crack structure by class, two images are created at this point. The original MAT image is separated into a MAT image of delamination cracks, and, likewise, transverse bundle cracks.

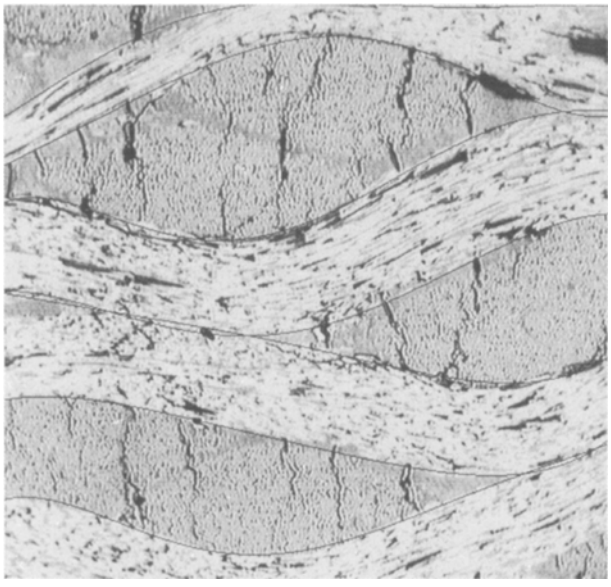

Figure 6 Illustration of the function fits made to identify the boundaries between longitudinal and transverse fibre bundles. The black lines are the seventh-order polynomial fits to the boundaries.

4.2. Number of cracks per unit area

Cracks can be automatically identified and labelled as individual cracks. Labelling is accomplished by tracing along each MAT crack line, including all branches, until all parts of the crack have been traced. The crack is changed to a uniform and unique colour during the process of tracing, thereby making each crack an easily identified individual. Once the labelling is done it is straightforward to count the number of cracks. The ability to identify cracks as individuals is used in several of the other measurements described below.

4.3. Crack length

Crack length is taken as the length of the MAT line representing the crack. The measured length, as presently implemented, includes all branches of the crack, if any.

Measurement of line length in a digital image is not as straightforward as it might first appear. There is a discretization error that accumulates when a diagonal

line is represented as a set of steps. It can be shown that the maximum absolute error is 11.70%, and the apparent length is always greater than the actual length. To centre the error so that the average measured crack length is correct, each individually measured crack length is multiplied by 0.9447. The resulting crack length data will have a maximum error of $\pm$ 5.85%, with a typical error of $\pm$ 2.07%.

Another difficulty in obtaining accurate crack-length statistics is the counting bias imposed by the higher probability of counting short cracks compared to long cracks. Images generally have cracks that extend beyond the field of view; the lengths of these cracks cannot be used in the analysis because their lengths are unknown. Compensation of the crack-length counting bias is accomplished by using an "effective count" correction [5]. The effective count is simply defined as the inverse of the probability that the crack will not extend off the screen. The unbiased number of cracks of a given length is estimated by summing the effective counts. Since cracks can be curved or have branches, the effective count must be based on the horizontal and vertical Feret's dimensions of each crack. (A Feret dimension is a projected length. It is often convenient to define a Feret box, which is the size of the box within which an object will just fit.)

Figs 8 and 9 show the crack length distribution of the carbon–carbon sample; the cracks have been separated by class. Also shown in the figures are crack density measurements. The histograms show two distributions. The measurements were made on the same material, but specimens were excised from different regions. The material was part of a fractured shear-test sample; one of the crack morphology specimens was cut from a region near the gauge section and the other from a region near the gripped section, hence the designation "stressed" and "unstressed". Clearly the stress history of these specimens is not well defined. The data are intended only to demonstrate crack quantification capabilities.

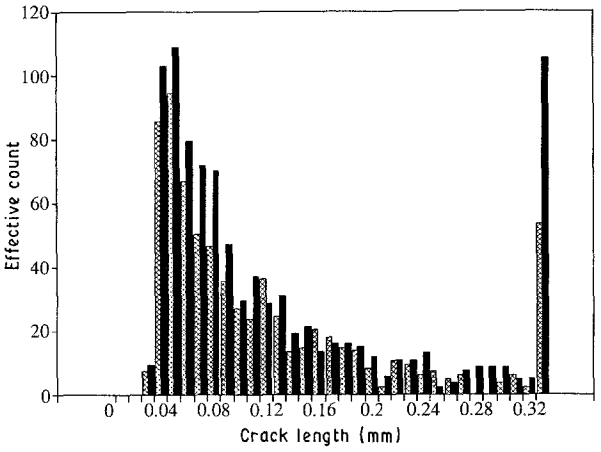

Figure 8 Transverse bundle crack length data from the example material. See text for a discussion of the stressed versus unstressed distinction. ▩ Unstressed: average = 0.132 mm, standard deviation 0.152 mm, sample size = 711, crack density = 18.69 mm^{-2}. ■ Stressed: average = 0.158 mm, standard deviation = 0.206 mm, sample size = 921, crack density = 26.87 mm^{-2} (44% increase).

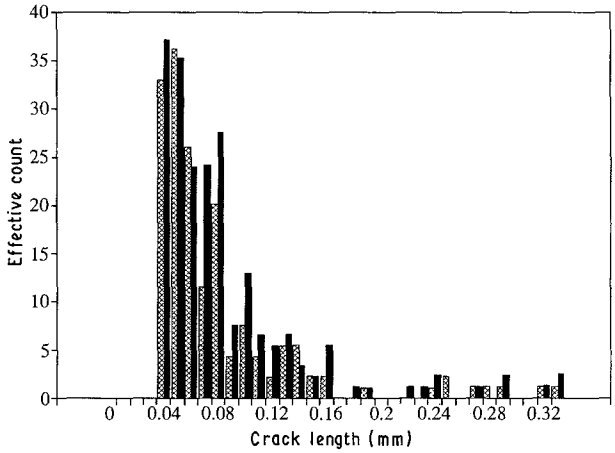

Figure 9 Delamination crack length data from the example material. See text for a discussion of the stressed versus unstressed distinction. ▩ Unstressed: average = 0.077 mm, standard deviation = 0.059 mm, sample size = 171, crack density = 4.49 mm^{-2}. ■ Stressed: average = 0.080 mm, standard deviation = 0.058 mm, sample size = 214, crack density = 6.26 mm^{-2} (39% increase).

The figures show, for example, that there is about four times as much transverse bundle cracking as delamination cracking, that both crack densities have increased substantially in the stressed specimen, and that the average length of the transverse bundle cracks has increased due to the load history.

4.4. Crack spacing

Crack spacing is often of interest in damage mechanics models (cf. [6]). In the case of carbon–carbon materials the spacing of transverse bundle cracks within a single ply is of particular interest, and this is the measurement that will be described. In this case, crack spacing is defined as the in-plane (horizontal in the

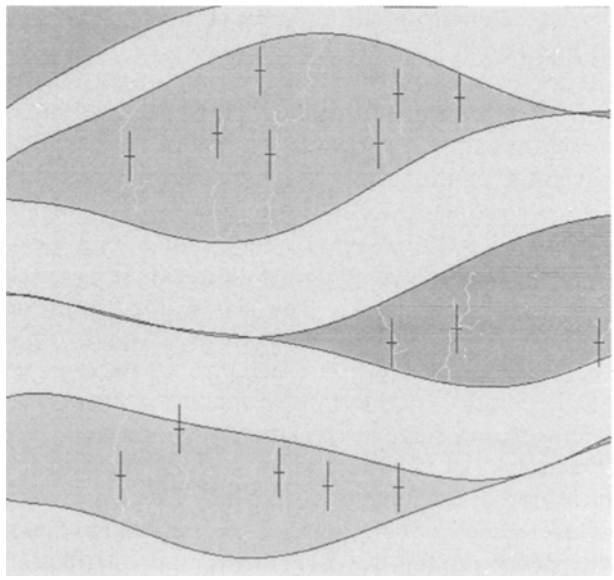

Figure 10 Preparation for measuring the in-plane spacing between transverse bundle cracks. The image shows the calculated centroids of the MAT cracks, and also shows the computer recognition of the individual laminae, so that the ply ownership of each crack can be determined. Cracking of the longitudinal yarns is not of interest in these measurements, so these cracks have been discarded.

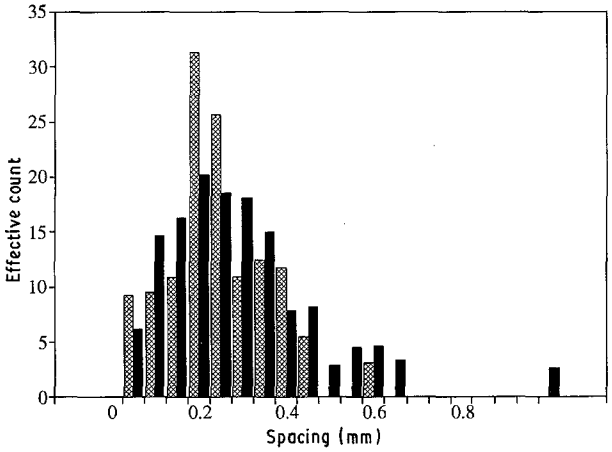

Figure 11 Data on crack spacing of transverse bundle cracks, corrected for the counting bias as discussed in the text. ▩ Unstressed: average = 0.220 mm, standard deviation = 0.115 mm, sample size = 129. ■ Stressed: average = 0.266 mm, standard deviation = 0.175 mm, sample size = 142. Feret size > 0.125 mm × 0.073 mm.

image) distance from one crack centroid to the adjacent crack's centroid.

Crack spacing measurements are begun by determining the centroid of each MAT crack. It is also necessary to determine which crack belongs to which ply. Both stages are automated. Calculation of the centroid is straightforward. Identification of the ply ownership of each centroid is aided by the interface boundary functions used in the classification stage. Fig. 10 shows the highlighted centroid for each MAT crack with Feret dimensions greater than 125 μm × 73 μm; the smaller cracks have been discarded because these data were intended to serve an analysis that focused on the larger cracks. Here again compensation must be made for the counting bias that will favour counting small spacings. This is done by using an effective count correction similar to the correction described for the crack length measurements. Crack spacing data from the example material are given in Fig. 11.

4.5. Crack orientation

Crack orientation is defined as the average angular deviation of the crack with respect to a reference frame. To compute crack orientation, a MAT crack is considered a set of (x, y) points and a best least-squares line through the centroid of the MAT crack is fitted to these points. The line is fitted using an "eigenvector fit" technique, which gives equal weight to x and y deviations from a line through the centroid of the points [7]. The slope of the line is then translated into an angular deviation from the reference direction. Fig. 12 shows short vectors representing measured orientation for each crack. The distribution of microcrack orientations for the example material are shown in Fig. 13. The orientation distribution reveals that most of the new cracks formed at an angle of 15–40° with respect to the warp yarn direction.

Finally, it is noted that width measurements can also be obtained from the raw data as described above; however, the measures have not yet been implemented.

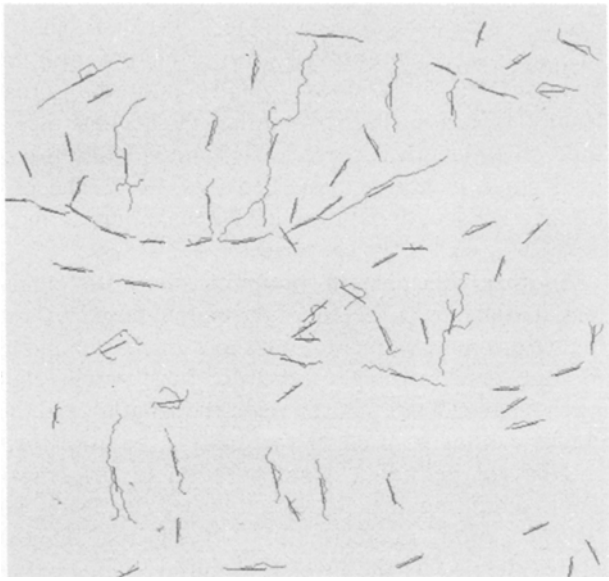

Figure 12 Measurement of crack orientation. Image of the automatically determined orientation vectors superposed on the MAT crack image. The cracks in this image have not been separated into delamination and transverse bundle cracks.

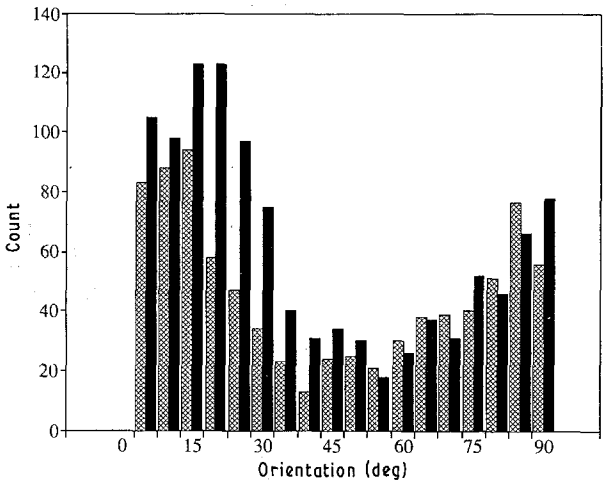

Figure 13 Crack orientation data from the example material. These data include both delamination and transverse bundle cracks. ▩ Unstressed: average = 40.92°, standard deviation = 30.43°, sample size = 842. ■ Stressed: average = 36.60°, standard deviation = 28.71°, sample size = 1113.

4.6. Note on hardware

The image processing required to make these measurements is substantial. The work described above was done with Imaging Technology, Inc. 150 series image processing hardware connected to a Silicon Graphics 4D25 workstation. Hardware control software and low-level image-processing software was purchased from G. W. Hannaway and Associates, Inc. The processing required in-house writing of 5700 lines of C-code. The approximate time to run all of the crack quantification routines on a single image is about 7 min. The processing requirements are substantially greater than current PC-based image processing systems can comfortably handle, but the gap is closing.

5. Limitations of the measurements

The crack structure data have several limitations that must be understood to enable proper interpretation. The limitations are related to size detection limits, processing steps leading to the MAT representation of the cracks, specimen preparation, and taking a two-dimensional view of a three-dimensional microstructure.

5.1. Size detection limits

The detectable crack size will, of course, be dependent on the microscope magnification used to obtain the original image. This magnification is chosen to reveal the structural features of interest.

For straight cracks the maximum detectable crack length is approximately the length of one side of the image. Materials that have cracks with curves and branches may result in lengths that are considerably longer than this. More precisely, the maximum detectable crack length has a maximum Feret diameter equal to the image side length.

The minimum detectable crack length is limited by the resolution in the digital image. In the technique described above, the minimum detected crack length was somewhat artificially limited, in the examples, to 10 pixel units. This restriction was necessary to eliminate spurious medial axis branches and other "noise" in the image. This restriction has the advantage of clearly defining the lower limit of detected crack length.

A more critical limitation to consider is the minimum detectable crack width. Again, this is usually limited by the digital image resolution rather than the microscope resolution if proper attention is given to set-up of the microscopy. In the image processing strategy described above, a crack is detected if a pixel is black after thresholding. The conditions under which this will occur can be found by considering Fig. 14. An actual crack may straddle two pixels in the digital image. The grey-scale value of each pixel is the average of the light intensity within the pixel area. Given a threshold value of C_t, a black pixel will remain in the image if the crack width is

$$w = 2k\frac{C_b - C_t}{C_b - C_c} \quad (1)$$

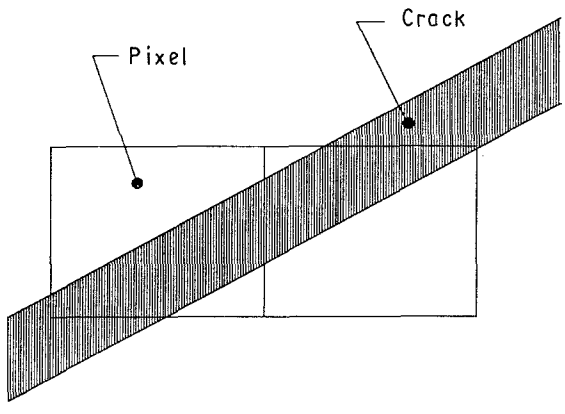

Figure 14 Sketch illustrating how the minimum detectable crack width is determined.

where C_c is the crack grey level, C_b is the background grey level and k is a magnification-dependent conversion factor between pixel units and length units. This is a worst-case estimate; it is based on a vertical crack exactly straddling two pixels. On the other hand, this analysis does not consider uncertainty in camera operation, or other minor errors such as edge diffraction. Overall, this is a reasonable estimate of minimum detectable crack width. Clearly, better contrast between cracks and background results in better detectability; microscopy and sample preparation techniques can help in this effort.

To use this relationship in practice, several of a series of measurement images are polled for the average crack grey level (by looking at a wide crack), yielding C_c. The average intensity of an entire image is taken as a measure of C_b.

In the example data given here, using a 10× objective on a simple optical microscope, and no sample preparation beyond standard metallographic polishing, $w = 4.7\,\mu m$. (For a sense of scale compare with a fibre diameter which is about 7 μm.)

5.2. Uncertainty in processing to a MAT representation

A source of uncertainty in the data occurs in the steps leading to the MAT representation of the crack structure. As noted, it is necessary to chose a threshold value to segment the image, a crack-segment connecting length, a contour smoothing parameter, and a spurious MAT branch threshold length. All of these choices become, unavoidably, a matter of judgement. In practice it has been possible to make judgements which appear to give a good representation of the crack structure. Judgements are made on the basis of comparing original images to the MAT images. Sensitivity studies are also used – for example, looking at the measured average crack length as a function of systematically varied threshold levels. Such studies typically reveal a "plateau region" in which the measured values are not sensitive to variations in choice of processing parameter. Once the processing parameters are chosen it is possible, fortunately, to make quantitative estimates of the detection limits, as discussed above.

Making relative comparisons can avoid some of the uncertainty inherent in absolute measurements. Use of image processing techniques provides excellent reproducibility. This reproducibility can be used to good advantage by designing experiments which rely on relative comparisons of microcrack structure. For example, crack structure can be quantified in similar specimens that have had different manufacturing, stress, or thermal histories. Care is taken to use the same processing parameters to make all measurements. It should be noted that this also requires attention to details such as overriding automatic gain and black-level adjustments on typical video cameras, and quantitative control of microscope illumination intensity.

5.3. Specimen preparation

Concern about specimen preparation is part of any crack structure measurement. Damaging the specimen during preparation must be avoided, but it is difficult to assess such damage. In the carbon–carbon material used as an example in this paper, experiments suggest that preparation does not create detectable damage. Specimens impregnated with epoxy to fill existing cracks did not reveal new cracks after preparation. A single specimen that went through a series of polish/measurement steps did not show a gradient in measured crack morphology, again suggesting that preparation did not create damage, at least not damage extending more than about 100 μm (the polish step size) below the surface. In addition, the ability to discern differences in crack structure between, for example, stressed and unstressed specimens that have received identical preparation supports a similar conclusion. Experience with metallographic polishing of the specimens also develops an understanding for what types of damage are caused by preparation, and what damage is inherent in the specimen. Proper preparation is, of course, dependent on the material being studied.

5.4. A planar view of a three-dimensional crack

The work described above characterizes a planar section of a three-dimensional (3D) crack structure. While the measures of crack structure made from sectional views can be valuable descriptors of morphology, it is necessary to remain aware of their possible limitations in describing the full picture.

The adequacy of two-dimensional (2D) data depends on the material and on how the data are used. Section data can frequently prove adequate. For example, composite materials often have a symmetry that allows approximating the structure as 2D. Further, most micromechanics models are limited to 2D approximations.

Sectional data can, in principle, be used to obtain information about 3D structure. This is the fundamental goal of stereological methods. Unfortunately these methods generally require an *a priori* knowledge of feature shapes – information typically not available for microcracks. Sometimes reasonable assumptions about feature shape can be made and can lead to the extraction of 3D structure data. For example, assuming that transverse bundle cracks are flat and have a perimeter equal to the bundle perimeter can lead to an estimate of volumetric crack density and a spherical distribution function of crack orientation.

This discussion points to a need for at least some 3D information on structure. It is possible to reconstruct a 3D structure using a series of parallel sections, and this is planned for future work.

6. Conclusions

The techniques developed here are capable of providing a rich, quantitative description of microcrack structure. A key feature of the approach has been the application of digital image processing to make the measurements. The abstraction of the crack structure to a set of medial axis lines is a fundamental part of the strategy. The use of digital image processing makes possible statistically significant, time-effective, reproducible measurements and can greatly expand the availability of quantitative data on microcrack morphology.

Techniques for classifying cracks, and measuring number, length, spacing and orientation have been developed. Other measures of crack morphology may need to be invented; the approach developed provides flexibility to adapt to the pursuit of other types of required crack data. There are limits in the crack structure measurements – related to size resolution, choice of processing parameters, specimen preparation, and planar views – which must be recognized for proper use of the data. The techniques used to make the measurements continue to be refined with experience.

Example images and data from a carbon–carbon composite have illustrated the measurements. Extension of the measurements to other brittle-matrix composites is possible with refinement of details particular to the material. Some of the ideas appear to be useful if extended to the measurement of cracking in coatings.

A discussion of how these crack structure measurements can be used exceeds the scope of this paper. Certainly microstructural modelling efforts can benefit from such data, as input and for experimental verification of model predictions. Crack quantification can also be useful in the study of processing schedules, quality control and structural-life assessment.

Acknowledgements

This work was made possible by ONR contract N00014-90-J-1908. The authors thank Dr L. H. Peebles and Dr S. G. Fishman, ONR Scientific Officers, for their encouragement and support. Mr Julius Jortner, of Jortner Research and Engineering, Inc., provided valuable discussions. Dr John Moosebrugger provided valuable comments on the manuscript.

References

1. J. JORTNER, *Carbon* **24** (1986) 603.
2. S. W. YURGARTIS, B. S. MACGIBBON and P. MULVANEY, "Source Code for Quantification of Microcracking, June 1991", Mechanical and Aeronautical Engineering Dept. Report No. 234 (Clarkson University, Potsdam, New York).
3. R. T. DEHOFF and R. T. RHINES, in "Quantitative Microscopy" (McGraw-Hill, New York, 1968).
4. H. BLUM, in Proceedings of Symposium on Models for Perception of Speech and Visual Form, edited by Weiant Whaten-Dunn (MIT Press, Cambridge, Mass., 1967).
5. J. C. RUSS, "Computer Assisted Microscopy: The Measurement and Analysis of Images" (Plenum, 1990).
6. R. TALREJA, in "Advances in Fracture Research", Vol. 3 (1989) pp. 2189–2198.
7. R. O. DUDA and P. E. HART, in "Pattern Recognition and Scene Analysis" (Wiley, New York, 1973).

Received 2 September 1991
and accepted 24 March 1992